Heliyon 10 (2024) e33411

Contents lists available at ScienceDirect

Heliyon

journal homepage: www.cell.com/heliyon

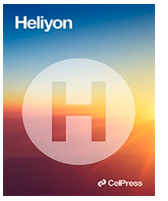

Research article

The common pathogenesis of nodular goiter in both sexes: An exploration into gene expression and signaling pathways

Xiangju Gao [a], Jie Gao [b], Ya Sun [c], Jing Zhao [b], Li Geng [b], Changlin Wang [a], Mingqi Qiao [b], Jieqiong Wang [d,*]

[a] *Research and Innovation Team of Emotional Diseases and Syndromes in Shandong University of Traditional Chinese Medicine, Jinan, 250355, China*
[b] *School of Chinese Medicine, Shandong University of Traditional Chinese Medicine, Jinan, 250355, China*
[c] *Institute of Traditional Chinese Medicine Innovation, Shandong University of Traditional Chinese Medicine, Jinan, 250355, China*
[d] *Emotional Disease Syndrome Liver Storage Pharmacological Young Scientific Research Innovation Team in Shandong University of Traditional Chinese Medicine, Jinan, 250355, China*

ARTICLE INFO

Keywords:
Thyroid goiter
Both sexes
Pathogenesis
Gene expression
Signaling pathways

ABSTRACT

The past few years have witnessed an increasing incidence of nodular goiter (NG), with a well-documented higher prevalence in females than males. This gender disparity has led research to focus primarily on female subjects, potentially overlooking common pathogenic mechanisms in both sexes. In this study, we investigated the shared pathogenesis of NG in males and females. Utilizing a rat model and RNA sequencing, we identified differentially expressed genes associated with the disease. We further validated these findings in normal human thyroid cells and human papillary thyroid cancer cells. A randomized experiment was conducted with equal numbers of male and female rats divided into control and NG model groups. The NG model was established using propylthiouracil and various assessments such as thyroid ultrasonography, thyroid index, thyroid function, and thyroid histology were performed. Transcriptome analysis revealed numerous upregulated and downregulated genes in both male and female model groups. Key genes like *KDR*, *FLT1*, *PDGFB*, and *CAV1*, and pathways including PI3K-Akt, MAPK, Ras, fluid shear stress and atherosclerosis, calcium signaling, and Rap1 signaling pathways were linked with the disease. Western blot and immunofluorescence analysis confirmed these findings, which were further supported by cell-based experiments. In conclusion, our findings suggest that abnormal expression of specific genes and pathways leading to irregular cell growth, blood vessel formation, and inflammation may be common factors in the pathogenesis of NG in both males and females.

1. Introduction

Goiter, defined as the abnormal enlargement of the thyroid gland, is commonly observed in various thyroid disorders, including endemic goiter, autoimmune thyroiditis, Graves' disease, nodular goiter, thyroid cancer, and granulomatous and infiltrative thyroid

* Corresponding author. Shandong University of Traditional Chinese Medicine, Jinan, 250355, China.
E-mail addresses: 61060469@sdutcm.edu.cn (X. Gao), jiegaosdutcm@163.com (J. Gao), 60230051@sdutcm.edu.cn (Y. Sun), 2021110007@sdutcm.edu.cn (J. Zhao), 2021110024@sdutcm.edu.cn (L. Geng), 2021100008@sdutcm.edu.cn (C. Wang), 2021110031@sdutcm.edu.cn (M. Qiao), jieqiong2016@126.com (J. Wang).

https://doi.org/10.1016/j.heliyon.2024.e33411
Received 6 November 2023; Received in revised form 20 June 2024; Accepted 20 June 2024
Available online 21 June 2024

diseases. While the etiologies and pathogenesis of these diseases differ, dysregulation of thyroid-stimulating hormone (TSH) secretion may play a role in the majority of these conditions [1]. Since the inception of the World Health Organization's global iodized salt program in 1993, iodine deficiency, a principal cause of goiter, has been effectively addressed, reducing the global incidence of goiter to an estimated 7 % [2]. In China, this rate has decreased further to roughly 2.4 % [3]. However, in recent years, the incidence of nodular goiter has exhibited a marked upward trend; prevalence rates have soared to between 24.4 % and 44.02 %. With an estimated 5 %–15 % of thyroid nodules being tumors [4], nodular goiter has become a significant global public health issue.

Nodular goiter is a type of goiter primarily caused by insufficient thyroid hormone secretion, which leads to an increase in thyroid volume. Over time, the thyroid gland may undergo abnormal follicular cell proliferation, resulting in the formation of single or multiple nodules. While most nodules are benign, a small percentage can progress to thyroid carcinoma, posing a health risk to patients and placing a burden on healthcare resources. Current research suggests that the development of nodular goiter may involve a complex interplay of environmental, genetic, and physiological factors. These factors include iodine deficiency, specific gene mutations, and dysregulated sex hormones. Additionally, autoimmune thyroid disorders, chronic thyroid stimulation or inflammation, and factors like age and sex may also be associated with the manifestation of nodular goiter [5]. At the genetic level, alterations within the *RET* gene are linked to the pathogenesis of multiple endocrine neoplasia type 2 (MEN2) [6]. Similarly, mutations in the *BRAF* and *RAS* genes are frequently observed in thyroid papillary carcinoma [7]. Abnormalities in *PTEN* and *APC* genes have also been implicated in the development of thyroid pathologies [8], while variations in the *DICER1* gene have been associated with an increased susceptibility to thyroid tumors [9].

Recent studies demonstrate that nodular goiter is more prevalent in women than in men [10]. Furthermore, substantial differences exist in the pathogenesis of nodular goiter between genders. These variations could be linked to disparate physiological and hormonal contexts. For instance, the hormonal milieu in women during their reproductive years and menopause influences thyroid function [11]. Additionally, estrogen is known to facilitate thyroid cell proliferation and deterioration [12]. However, diagnosis in male patients typically occurs at a later stage, with a more aggressive disease course [13]. Moreover, there is an increased risk of nodular goiter progressing to malignancy, with a heightened likelihood of central neck lymph node metastasis [14,15].

Despite the evident gender-based disparities in the pathogenesis of thyroid nodules, it remains imperative to elucidate and examine the underlying mechanisms common to both sexes in the development of thyroid nodules. Indeed, the identification of shared mechanisms could uncover fundamental biological processes driving the formation of thyroid nodules. A comprehensive understanding of these processes is likely to inform the creation of more efficacious preventive and therapeutic approaches. For instance, environmental influences could significantly contribute to the development of thyroid nodules across genders. Likewise, genetic

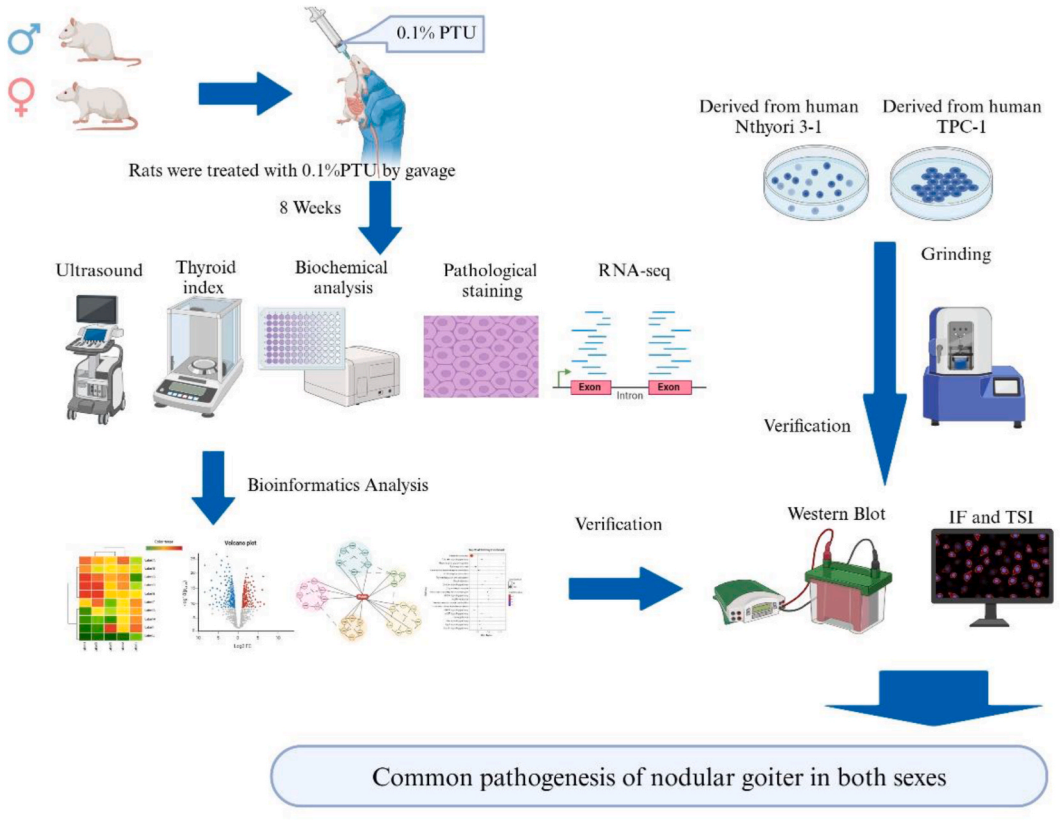

Fig. 1. Flowchart outlining the experimental design and methodology of this study. Created With BioRender.com.

predispositions, immunological reactions, and specific lifestyle choices might similarly impact the emergence of thyroid nodules in both men and women.

Given the limited research on the common pathogenic mechanisms between genders and the rising prevalence of nodular goiter [10], further investigation in this area is crucial. Elucidating the causative factors and underlying pathology of this condition holds promise for improving the accuracy of diagnosis and treatment, ultimately leading to better patient outcomes. Rigorous research efforts could contribute to a decline in disease incidence, improved patient survival rates, and enhanced quality of life for individuals affected by nodular goiter.

This research is based on the principle that TSH is the main factor driving thyroid gland growth [5]. To investigate this, propylthiouracil (PTU) was chosen for oral administration. It is now understood that PTU effectively reduces thyroid hormone production, leading to a significant increase in TSH levels and resulting in pathological thyroid hyperplasia, thus creating a rat model of nodular thyroid hyperplasia [16–18]. In our study, RNA sequencing (RNA-seq) was used to investigate key genes involved in the pathogenesis. Studies show that progression to thyroid papillary carcinoma (TPC) is quite common in individuals with nodular goiter, with over half of PTC cases reported to have a history of nodular thyroid complications [19–21]. Due to these findings and the inherent challenges of obtaining cells from human nodular goiters, cells from human papillary thyroid carcinoma were selected as a suitable substitute. These TPC cells, along with normal human thyroid cells, were instrumental in validating the accuracy of the rat model outcomes and ensuring the reliability of the conclusions drawn (Fig. 1).

2. Materials and methods

2.1. Animals

Sixty 6–8 week old male and female SPF-grade Wistar rats (150–180 g) were purchased from Beijing Charles River Laboratory Animal Technology Co., Ltd. [SCXK (Beijing) 2021–0011] and housed in the Laboratory Animal Center of Shandong University of Traditional Chinese Medicine [SYXK (Shandong) 2022–0009] with free access to water and food. The facility maintained a 12/12 h light/dark cycle, 23 ± 1 °C temperature, 50–60 % humidity, and noise ≤60 Db. All procedures were approved by the Animal Welfare Ethics Review Committee of Shandong University of Traditional Chinese Medicine (SDUTCM20230628001), and the animals were treated according to the 3 R principle.

2.2. Cells

Prior to initiating cellular investigations, human normal thyroid cells (Nthyori 3–1) and human papillary thyroid carcinoma cells (TPC-1) were obtained from Suzhou Haixing Biotechnology Co., Ltd. and subjected to Short Tandem Repeat (STR) profiling for cell line authentication (refer to Supplementary Material 1). Following this verification, both cell types were cultured in their designated complete media: FBP-C520 medium for the Nthyori 3–1 cells and TCH-G381 medium for the TPC-1 cells. These cells were maintained in a humidified CO_2 incubator set at 37 °C and 5 % CO_2 (Thermo Fisher Scientific, USA), Both the cell lines and their respective culture media were obtained from Suzhou Haixing Biotechnology Co., Ltd (Jiangsu, China).

2.3. General observations

Daily observations of the rats were documented, including their behavior, mentation, food and water intake, defecation patterns, and fur condition. Following the completion of the experimental modeling, the thyroid glands were harvested, and their absolute weight and weight-to-body weight ratio were determined.

2.4. Model preparation

Sixty Wistar rats were divided into four equal groups (n = 15/group) stratified by sex. The groups were designated as female control (F Control), male control (M Control), female model (F model), and male model (M model). To induce a nodular goiter model, the methodology described by Tamura et al. [22] was employed. During the modeling phase, rats in the model groups received daily intragastric administration of 0.1 % PTU at a dose of 100 mg/kg body weight for eight consecutive weeks. Conversely, rats in the control groups received an equivalent volume of saline via intragastric gavage over the same period. PTU was sourced from Shanghai ZhaoHui Pharmaceutical Co., Ltd. (Shanghai China), and physiological saline was obtained from Cisen Pharmaceutical Co., Ltd. (Jining China).

2.5. Ultrasound examination

At the conclusion of the eight-week period, a thyroid gland examination was performed using a DAWEI P60 color Doppler ultrasound device (Dawei Electronic Equipment Co., Ltd., China) equipped with a high-frequency hockey stick probe (10 MHz). The cervical region of the rats was shaved to facilitate optimal probe contact. Subsequently, anesthesia was induced using isoflurane. The ultrasound examination commenced at the level of the mandible, with the probe systematically scanning the neck until the thyroid gland was visualized. Thyroid size was then measured, and the presence of nodules or calcifications was documented. Measurement packets within the ultrasound system were employed to calculate any statistically significant size differences between the groups.

2.6. Thyroid function test

Following an overnight fast (12 h) and water deprivation (2 h), the rats were weighed and isoflurane anesthesia. Blood samples were collected from the abdominal aorta. Serum was isolated by immediate centrifugation (3000 rpm, 15 min, 4 °C) and stored at −80 °C for subsequent analysis. Serum-free triiodothyronine (FT3), free thyroxine (FT4), and TSH levels were quantified using a commercially available enzyme-linked immunosorbent assay (ELISA) kit from Bioswamp Life Science Lab (Wuhan, China). Undiluted serum samples were used in the analysis, following the manufacturer's protocol for incubation with pre-coated, high-affinity target-specific antibodies. To ensure data reliability, all samples were assayed in duplicate. A standardized protocol was strictly followed for sample and reagent preparation to minimize variability and enhance measurement precision. This protocol included the generation of a fresh standard curve for each assay plate, enabling accurate quantification of the target proteins. Finally, the optical density of each well was measured at a wavelength of 450 nm using a SpectraMax iD5 (Molecular Devices, LLC, USA) spectrophotometer calibrated according to the manufacturer's instructions.

2.7. Histopathological examination

Following blood collection, thyroid tissues were meticulously dissected from both sides of the trachea in all rats. The harvested tissues were weighed, and the relative thyroid weight (thyroid weight/body weight) was calculated. One portion of each tissue was snap-frozen in liquid nitrogen and subsequently stored at −80 °C for future analysis. The contralateral portion was fixed in 10 % neutral buffered formalin (NBF) for 24 h, followed by progressive dehydration and paraffin embedding. Serial sections, 4 μm thick, were prepared using a Leica RM2255 microtome (Leica Microsystems, Germany) and stained with hematoxylin and eosin (HE). The sections were then examined under an Axio Observer 3 fluorescence microscope (Carl Zeiss Ltd., Germany) for evaluation of any potential pathomorphological alterations. All reagents were obtained from a commercial supplier (Biosharp Life Science, Hefei, China).

2.8. High-throughput sequencing technology of the whole transcriptome (RNA-seq)

Thyroid glands were rapidly frozen in liquid nitrogen and stored at −80 °C for subsequent RNA extraction. Total RNA was isolated from the thyroids of three rats per group using TRIzol® reagent (Magen). The purity and integrity of the extracted RNA were assessed using a Nanodrop ND-2000 spectrophotometer (Thermo Fisher Scientific, USA) by measuring the A260/A280 absorbance ratio. Additionally, RNA integrity was evaluated using an Agilent Bioanalyzer 4150 (Agilent Technologies, CA, USA) to determine the RNA integrity number (RIN value). Only RNA samples meeting quality criteria were used for library construction. Paired-end (PE) sequencing libraries were prepared following the manufacturer's instructions for the ABclonal mRNA-seq Library Prep Kit (ABclonal, China). Briefly, 1 μg of total RNA was used for mRNA purification with oligo(dT) magnetic beads. The purified mRNA was then fragmented in ABclonal First-Strand Synthesis Reaction Buffer. Subsequently, cDNA synthesis was performed using random primers and reverse transcriptase (RNase H) with the fragmented mRNA as templates. This was followed by second-strand cDNA synthesis using DNA polymerase I, RNase H, reaction buffer, and dNTPs. The double-stranded cDNA fragments were then ligated with adapter sequences to facilitate PCR amplification. The PCR products were purified, and library quality was assessed using an Agilent Bioanalyzer 4150. Finally, the libraries were sequenced on an Illumina NovaSeq 6000 sequencing platform with a paired-end read length of 150 base pairs (bp). The resulting sequencing data generated on the Illumina platform were used for bioinformatic analysis. All RNA isolation and library construction steps were performed by Shanghai Zhongke Xinsheng Life Biotechnology Co., Ltd.

2.9. Differential expression analysis, KEGG enrichment analysis, and key gene selection

Following generation on the Illumina platform, RNA sequencing data underwent quality control procedures. The raw sequencing data in FASTQ format were first processed using Perl scripts to remove adapter sequences and eliminate low-quality reads. Low-quality reads were defined as those containing a base quality value of $\leq$25 in more than 60 % of the read sequence or those with an N (indicating unknown base) ratio exceeding 5 %. This filtering process yielded high-quality, clean reads for subsequent analyses. HISAT2 software (http://daehwankimlab.Github.io/hisat2/) was employed to align the clean reads to a reference genome, generating mapped reads for further analysis. FeatureCounts (http://subread.sourceforge.net/) was then used to quantify the number of reads aligning to each gene. Gene expression levels were subsequently normalized using Fragments Per Kilobase Million (FPKM) values, which account for gene length. Differential expression analysis between groups was performed using DESeq2 software (http://Bioconductor.org/packages/release/bioc/html/DESeq2.html/), with a significance threshold set at $|\log2 \text{ fold change (FC)}| > 1$ and adjusted p-value (Padj) < 0.05 for identifying differentially expressed genes (DEGs). To elucidate common biological pathways potentially involved in both male and female models, the DEGs were subjected to Kyoto Encyclopedia of Genes and Genomes (KEGG) pathway enrichment analysis using the clusterProfiler R package. The results of this analysis were used to identify commonly enriched signaling pathways in both sexes. Subsequently, proteins associated with these commonly enriched pathways were used to construct a protein-protein interaction (PPI) network diagram. Key genes within this network were identified using the CytoNCA plugin (https://apps.cytoscape.org/) available within the Cytoscape software environment (version 3.8.2). The CytoNCA plugin employs a centrality metric to screen and identify genes with degree centrality >10.27, eigenvector centrality >0.00745, betweenness centrality

>3011.254, and closeness centrality >0.084711. These genes are considered to be central nodes within the network, potentially playing key regulatory roles.

2.10. Immunofluorescence assay (IF) and tissue section imaging (TSI)

Immunofluorescence staining was employed to assess the expression levels of target proteins within rat thyroid tissues. Briefly, formalin-fixed thyroid tissues were dehydrated, embedded, and sectioned to a thickness of 4 μm. Following deparaffinization, the sections underwent antigen retrieval using sodium citrate buffer (catalog no. D10252, Bioss, China), followed by overnight incubation with primary antibodies at these dilutions: KDR (no.#9698, Cell Signaling Technology, USA) at 1:800, FLT1 (no.bsm-52338 R, Bioss, China) at 1:100, CAV1 (no.bs-1453 R, Bioss, China) at 1:100, and PDGFB (no.bs-1316 R, Bioss, China) at 1:100. Subsequently, they were incubated with a CY3-conjugated secondary antibody (catalog no. bs-21928R-Cy3, Bioss, China) at a 1:500 dilution for 1 h at room temperature in a dark environment. Finally, the sections were stained with 4′,6-diamidino-2-phenylindole (DAPI) (catalog no. D-9106, Bioss, China) for nuclear counterstaining, mounted, and visualized using an Axio Observer 3 fluorescence microscope (Carl Zeiss Ltd., Germany). Target protein fluorescence was detected at an excitation wavelength of 528 nm, while DAPI fluorescence was detected at 461 nm. Image J software (National Institutes of Health, USA) was used to quantify the mean fluorescence intensity of the target proteins in each section. For near-infrared Western blot analysis, tissue sections were prepared in the same manner as for immunofluorescence staining. Following overnight incubation with primary antibodies, the sections were washed and incubated with an IRDye® 800CW secondary antibody (Gene Co., Ltd, HK) for 15 min. After additional washes, the sections were scanned using a LI-COR Odyssey® imaging system (Gene Co., Ltd, HK) at an emission wavelength of 800 nm.

2.11. Western blot

Total protein was extracted from thyroid tissues, Nthyori 3–1 cells, and TPC-1 cells using a RIPA lysis buffer supplemented with protease and phosphatase inhibitors. Protein concentration was quantified using a BCA protein assay kit (Glpbio, USA). Equal amounts of protein from each sample were separated by sodium dodecyl sulfate-polyacrylamide gel electrophoresis (SDS-PAGE) and subsequently transferred onto polyvinylidene fluoride (PVDF) membranes. The membranes were blocked with 5 % non-fat dry milk for 2 h at room temperature, followed by overnight incubation with primary antibodies diluted to the following concentrations: KDR (catalog no. 9698, Cell Signaling Technology, USA; 1:1000 dilution), FLT1 (catalog no. bsm-52338 R, Bioss, China; 1:1000 dilution), CAV1 (catalog no. bs-1453 R, Bioss, China; 1:1000 dilution, PDGFB (no. bs-1316 R, Bioss, China; 1:1000 dilution), and GAPDH (no. 10494-1-AP, Proteintech, China; 1:10000 dilution). The membranes were then washed and incubated with a goat anti-rabbit horseradish peroxidase (HRP)-conjugated secondary antibody (catalog no. bs-80295G-HRP, Bioss, China) at a 1:5000 dilution for 2 h at room temperature. GAPDH served as the internal loading control. Protein bands were visualized using an enhanced chemiluminescence (ECL) reagent (MilliporeSigma, Germany) and captured using a Tanon-4800 Multi imaging system (Tanon Life Science Co., Ltd, China). Band intensities were quantified using Image J software (National Institutes of Health, USA).

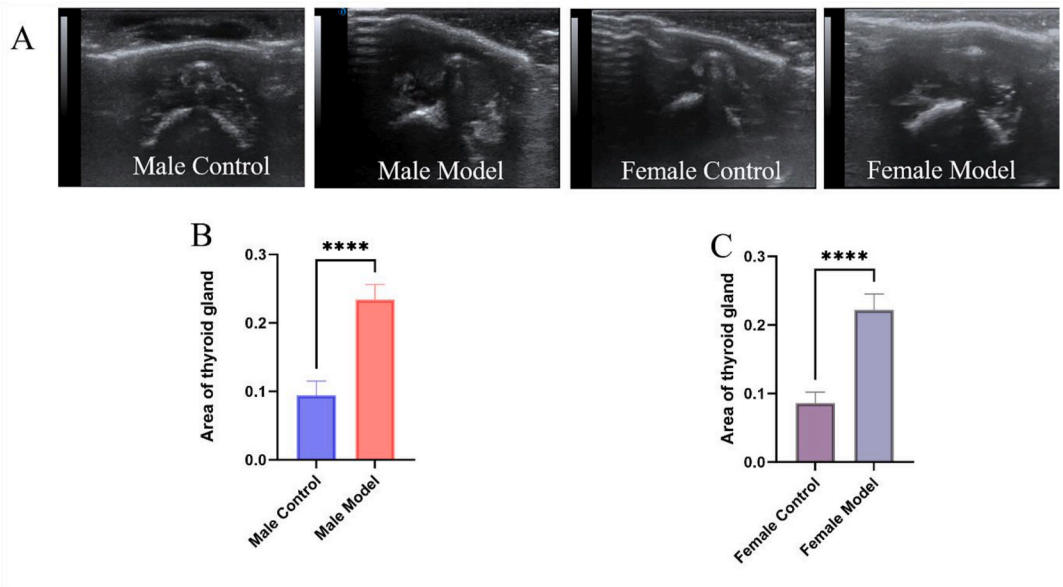

Fig. 2. Ultrasound imaging examination of the thyroid was performed after 8 weeks of PTU administration. (A) Following 8 weeks of intragastric PTU administration, the thyroid glands of rats in each group were assessed using ultrasound imaging. (B) Male and (C) Female after 8 weeks of PTU administration, thyroid ultrasound measurements were conducted on a random selection of 6 rats from each of the control and model groups. Data are shown as the mean ± SD (n = 6). ****$P < 0.0001$ vs. corresponding model group.

2.12. Statistical analysis

All data were presented as mean ± standard deviation (SD). Statistical analyses were performed using GraphPad Prism version 9.0 (GraphPad Software, USA). Pairwise comparisons were conducted using t-tests. A p-value of less than 0.05 was statistically significant.

3. Results

3.1. PTU used to establish a mouse model of nodular goiter

Ultrasound imaging findings were consistent with a diagnosis of nodular goiter in the model group.

The thyroid gland, located in the anterior-central region of the neck, is composed of two lobes connected by a narrow isthmus. On transverse ultrasound images, the normal thyroid typically appears horseshoe-shaped or butterfly-shaped. The thyroid capsule is typically visualized as a smooth, hyperechoic line. In the control group (comprising both sexes), rat thyroids exhibited uniform hyperechogenicity with visible anechoic tubular structures, consistent with blood vessels. Conversely, an ultrasound examination of the model group (including both sexes) revealed asymmetric enlargement of bilateral thyroid lobes containing abnormal tissue. These enlarged lobes displayed discrete nodules lacking a well-defined capsule and exhibiting irregular, ill-defined margins. Additionally, scattered, punctate, or elongated regions of fibrous hyperplasia with increased echogenicity were observed within the thyroid lobes (Fig. 2A). Quantitative ultrasound analysis demonstrated a significantly larger thyroid gland cross-sectional area in the model group compared to the control group (Fig. 2B and C).

3.2. Significant increase in thyroid weight and thyroid coefficient in the model rats

Thyroid imaging revealed a markedly larger volume in the model group compared to the other groups (Fig. 3A). The enlarged thyroids exhibited a dark red color, suggesting increased blood flow. The thyroid coefficient in the male model group displayed a trend toward being higher than the control group, but this difference was not statistically significant. Conversely, the female control group exhibited a significantly smaller thyroid volume compared to the model group (Fig. 3B and C).

3.3. TSH, FT3, and FT4 levels consistent with the diagnosis of nodular goiter

Following eight weeks of treatment with PTU, male rats exhibited a trend towards elevated serum TSH levels, although this increase did not reach statistical significance. Conversely, female rats displayed a statistically significant elevation in TSH levels compared to controls (Fig. 4A). In both male and female PTU-treated groups, serum levels of FT3 and FT4 were significantly decreased compared to control rats. These reductions in FT3 and FT4 were statistically significant (Fig. 4B and C).

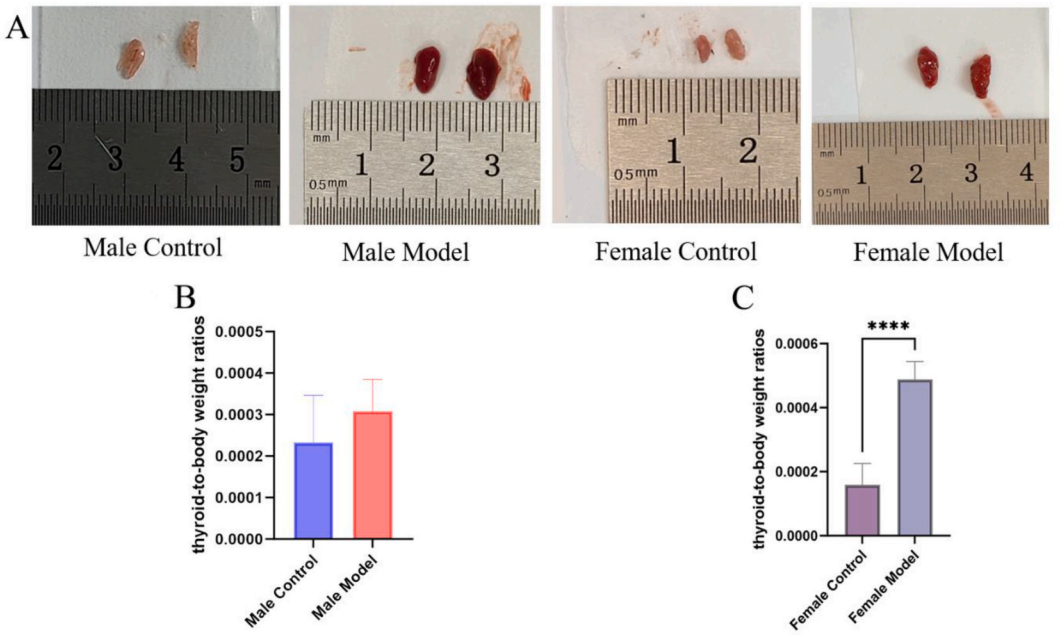

Fig. 3. Thyroid and thyroid coefficient changes at 8 weeks after modeling (A) After modeling, the thyroid tissue was removed, and 1 case in each group was randomly selected for filming. (B) Male and (C) Female, the thyroid to body weight ratio was compared with that of the corresponding model group. Data are shown as the mean ± SD (n = 6). ****$P < 0.0001$ vs. corresponding model group.

3.4. HE Staining of rat thyroid sections supports diagnosis of nodular goiter

Histological examination of HE-stained thyroid sections revealed normal follicular morphology in the control group. At 40x magnification, thyroid follicles displayed uniform size and even colloid distribution within the follicular lumens. The follicular epithelium was composed of a single layer of neatly arranged cuboidal cells with minimal observable capillaries (Fig. 5A and B). In contrast, the model group exhibited significant alterations in thyroid tissue architecture. Thyroid follicles displayed marked variation in size and shape. The follicular epithelium demonstrated prominent hyperplasia and a disorganized arrangement. The colloid appeared compressed and exhibited uneven distribution within the thyroid. Additionally, an increased number of capillaries and an expansion of loose connective tissue were observed. These histological findings are characteristic of nodular goiter, consistent with the prior ultrasound diagnosis (Fig. 5C and D). Based on the evaluation criteria established using these four parameters, this experiment successfully established a model of nodular goiter.

3.5. Functional annotation of nodular goiter using KEGG pathway and key gene analysis

Principal component analysis (PCA) revealed good consistency within the tested samples (Fig. 6A). Furthermore, differential gene expression analysis between the male and female model groups compared to the control group identified distinct expression patterns. In the male model group, 923 genes were upregulated, while 1088 genes were downregulated. Similarly, the female model group exhibited upregulation of 830 genes and downregulation of 1417 genes (Fig. 6B and C).

KEGG pathway enrichment analysis was performed to identify regulatory pathways associated with the DEGs. In the female cohort, 108 pathways were significantly enriched (Fig. 7A). Similarly, 95 pathways were enriched in the male cohort. Notably, 70 pathways were common to both sexes, encompassing a total of 1107 genes (Fig. 7B). A network analysis was employed to identify key regulatory genes within these commonly enriched pathways. This analysis utilized centrality metrics, including degree centrality, eigenvector centrality, betweenness centrality, and closeness centrality [23], to pinpoint key nodes within the network. Genes identified as key regulators included *KDR*, *Il6*, and *ALB* (Fig. 7C). To further elucidate the functional roles of these key genes, we examined their involvement in the top 20 enriched pathways shared by both sexes. This analysis revealed that KDR participated in seven pathways: the

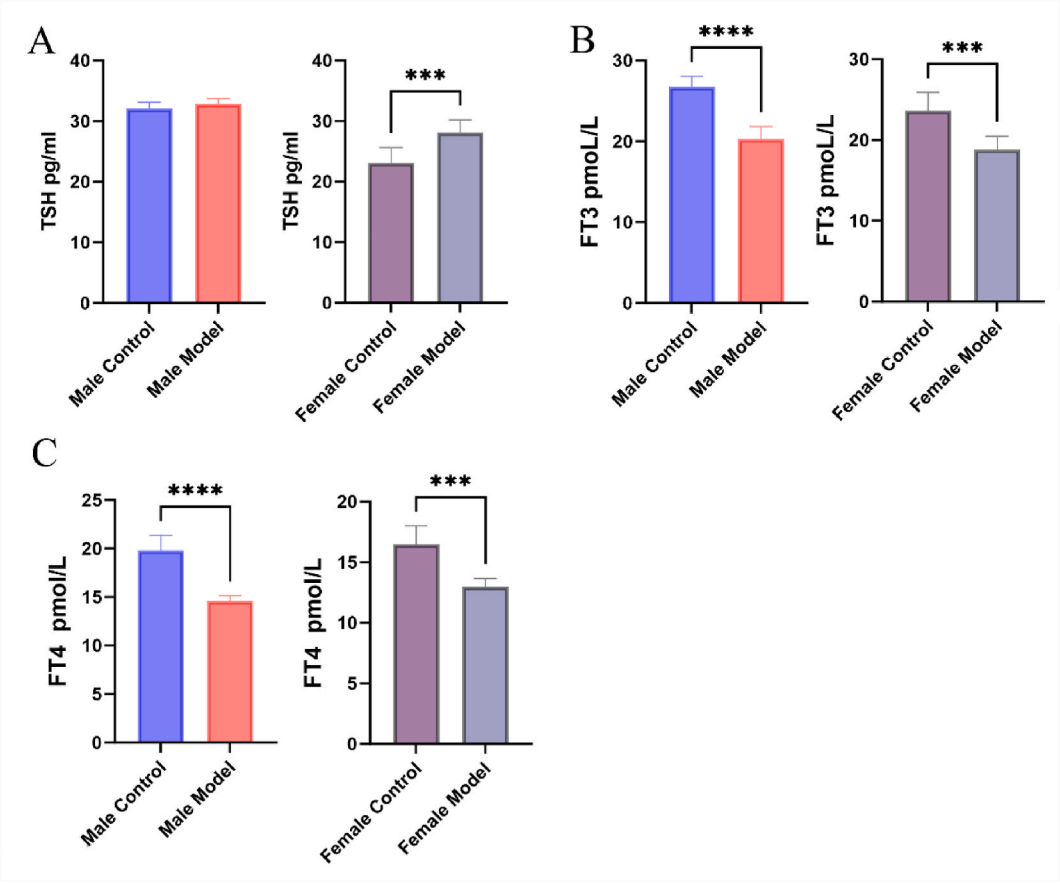

Fig. 4. Thyroid function test results. (A)TSH, (B)FT3 and (C)FT4 thyroid function test results after 8 weeks of modeling. Data are shown as the mean ± SD (n = 6). ***$P < 0.001$, ****$P < 0.0001$ vs. corresponding model group.

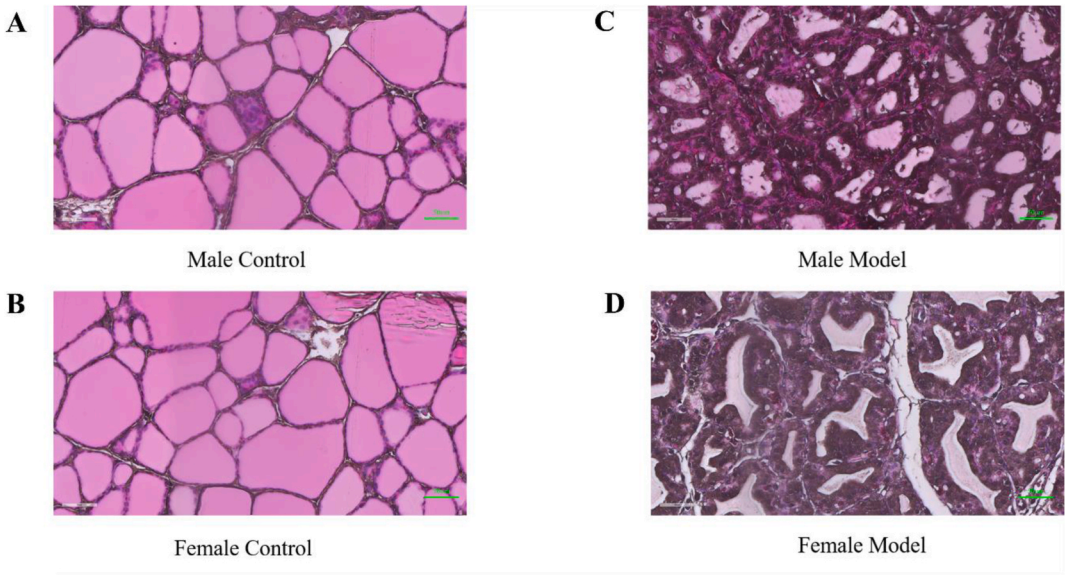

Fig. 5. Histopathological changes of thyroid in rats (stained with hematoxylin and eosin, scale bar = 50 μm, magnification × 400, n = 6) (A) Male and (B) Female, in the control group, thyroid follicles were uniform in size with an even distribution of colloid within the follicular lumens. (C) Male and (D) Female, in model group exhibited marked irregularities in thyroid tissue morphology, size, and follicle dimensions.

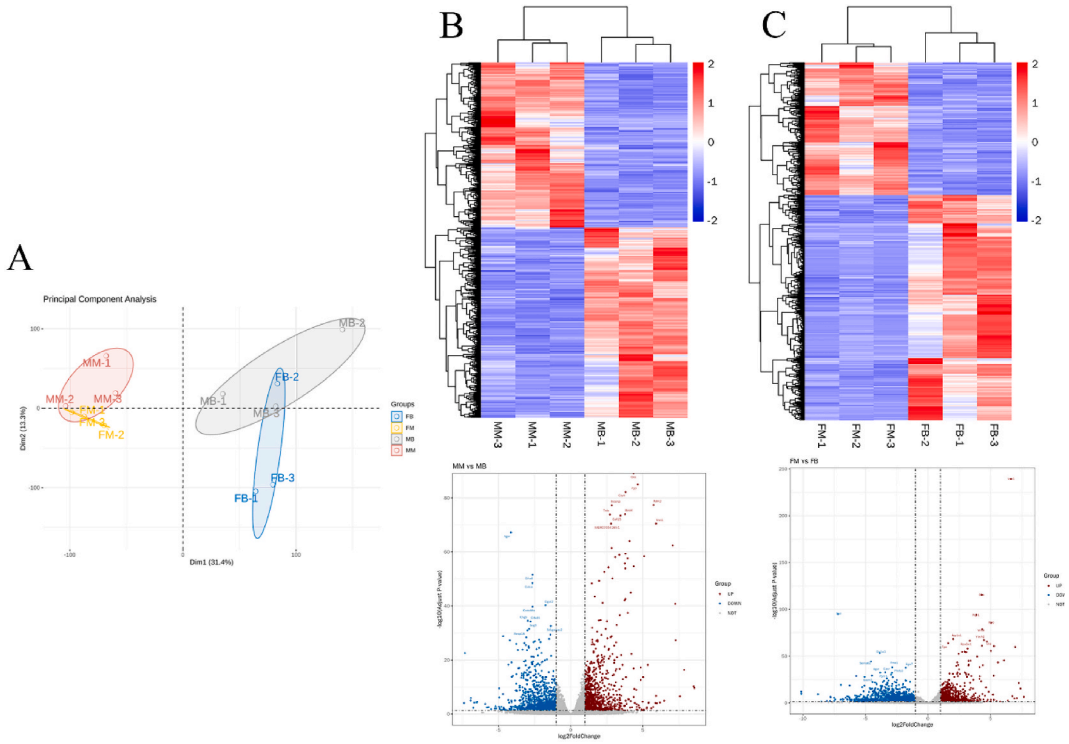

Fig. 6. Differential gene analysis by RNA-seq in nodular goiter (n = 3 rats per group) (A) The biological replication is good in the detected male and female control groups and model groups. (B) Hierarchical clustering thumbnail and differentially expressed gene volcano plot between the male model group and the male control group (up = 92; down = 1088). (C) Hierarchical clustering thumbnail and differentially expressed gene volcano plot between the female model group and the female control group (up = 830; down = 1417).

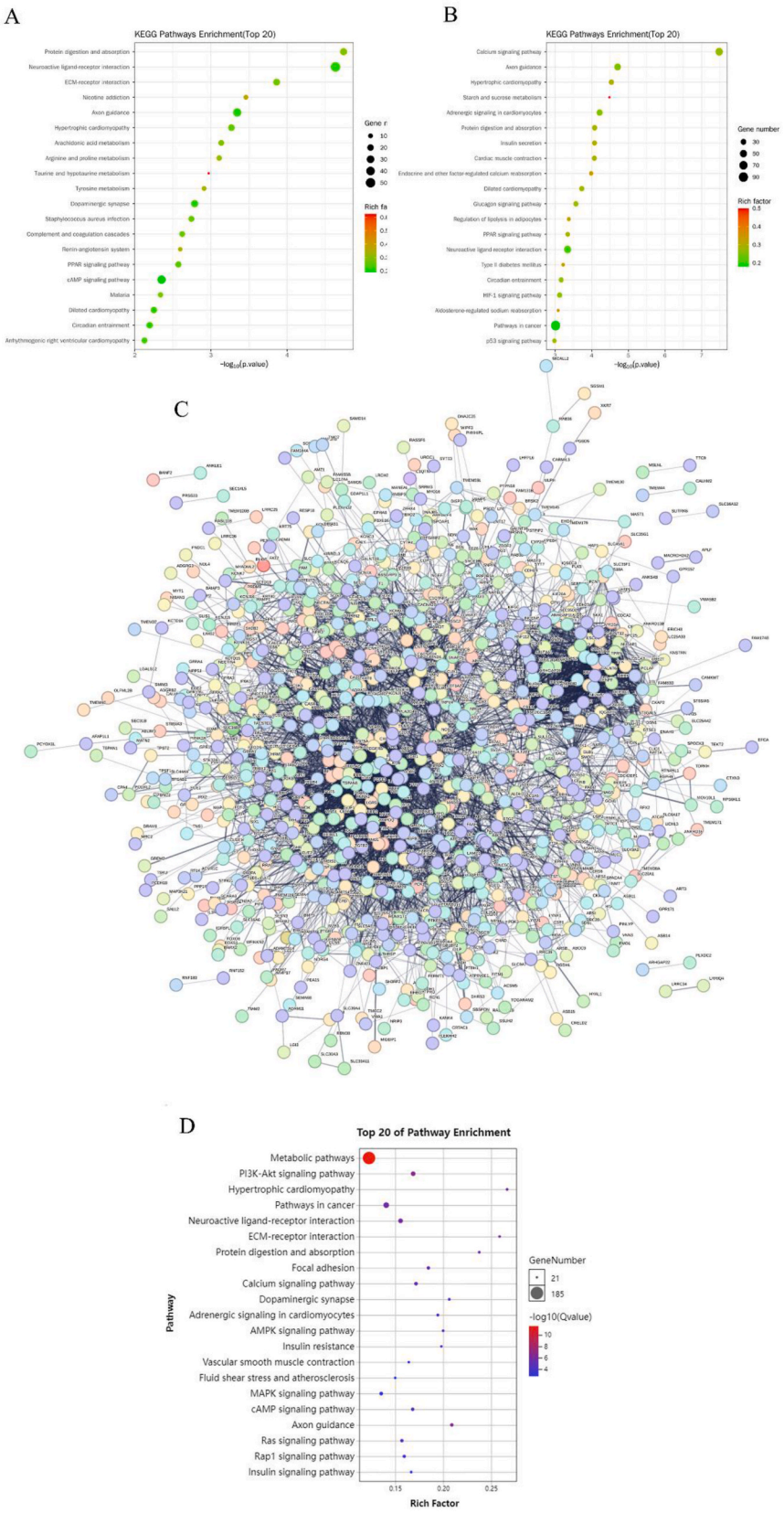

(caption on next page)

Fig. 7. RNA-seq enrichment analysis and gene analysis of nodular goiter (A) Top 20 pathways were obtained by KEGG enrichment analysis of male differentially expressed genes. (B) Top 20 pathways were obtained by KEGG enrichment analysis of male differentially expressed genes. (C) PPI map of genes included in the intersection of female and male KEGG pathways; (D) Top 20 KEGG pathways in the intersection of male and female.

PI3K-Akt signaling pathway, calcium signaling pathway, MAPK signaling pathway, Focal adhesion, Ras signaling pathway, Rap1 signaling pathway, and the pathway in Fluid shear stress and atherosclerosis (Fig. 7D). Conversely, IL6 was associated with three pathways, while ALB was not implicated in any of the top 20 pathways. Subsequent analysis of genes within these seven KDR-associated pathways revealed several crucial genes potentially involved in nodular goiter pathogenesis. These genes primarily included *KDR*, *FLT1*, *PDGFB*, and *CAV1*, and were predominantly enriched in six signaling pathways: PI3K-Akt signaling, MAPK signaling, Ras signaling, calcium signaling, Fluid shear stress and atherosclerosis, and the Rap1 signaling pathway.

3.6. Identification of key genes in the prioritized pathways

In summary, our findings highlight KDR as a pivotal protein within critical signaling pathways, alongside FLT1, PDGFB, and CAV1. These proteins likely play a significant role in the pathogenesis and progression of nodular goiter. To gain a more comprehensive understanding of the disease process, we investigated the expression levels of these key proteins within the implicated pathways (Fig. 8A). In the PTU-induced rat model of nodular goiter, protein expression analysis revealed an upregulation of KDR and FLT1, while PDGFB and CAV1 expression levels were downregulated. These changes were statistically significant (Fig. 8B).

3.7. In vitro validation in nthyori 3–1 and TPC-1 cell lines supports in vivo results

To investigate the translational potential of our findings in rats to the human context, we selected the Nthyori 3–1 cell line and the TPC-1 cell line, which closely resembles human thyroid nodules, for key protein validation. The validation results demonstrated significant upregulation of *KDR* and *FLT1* expression, while PDGFB and CAV1 expression levels were downregulated (Fig. 9). These observations in the human cell lines mirrored the trends observed in the in vivo experiments.

4. Discussion

The prevalence of thyroid nodules is on the rise, with detection rates in the general population reaching as high as 68 % [24]. This rise necessitates a deeper understanding of thyroid nodule pathology. The spectrum of thyroid nodule progression encompasses a range of presentations, varying from benign nodules and simple cysts to more concerning pathologic conditions. These conditions include nodular goiter, papillary carcinoma nodules, follicular carcinoma nodules, medullary carcinoma nodules, and diffuse goiter. Nodular goiter, characterized by the presence of one or more nodules within the thyroid gland, represents a significant public health concern. While most of these nodules are benign, a small but important subset may harbor malignancy. This potential for malignancy underscores the importance of appropriate evaluation and management of nodular goiter.

This study sheds light on the potential mechanisms underlying PTU-induced nodular goiter development. Our findings suggest that KDR-orchestrated dysregulation of signaling pathways might be a critical driver in nodular goiter initiation. Further analyses revealed that these pathways could potentially impact disease onset and progression through various mechanisms, including aberrant cellular proliferation, disrupted Ca^{2+} signal transduction, and abnormalities in both intracellular and intercellular communication. Notably, this study highlights three pathways that have received less attention in thyroid research: the fluid shear stress pathway associated with atherosclerosis, the calcium signaling pathway, and the Rap1 signaling pathway.

In recent years, thyroid research has benefited from a surge in investment and the continuous development of novel animal models [25]. Within China, studies investigating nodular goiter have primarily utilized rat models, employing various methods for their induction. A common approach involves triggering compensatory thyroid enlargement in rats by reducing iodine intake and elevating TSH levels. Several established models achieve this through different methods: Sun et al. used a pharmacological approach, administering PTU in drinking water for six weeks to female SD rats [26]. Conversely, Alayoubi et al. utilized an iodine-deficient diet [27], while Li et al. provided methimazole (MMI) in drinking water to male Wistar rats for 12 weeks [28]. In our experiment, we adopted Tamura's method [22] for model establishment, administering PTU via oral gavage for eight weeks. This approach ensured a precise and effective dose of medication, exceeding the efficacy achievable with self-consumption of PTU-containing water. Additionally, the extended modeling duration facilitated the development of thyroid hyperplasia, increasing the success rate of establishing a nodular goiter model.

Ultrasonography is a critical tool for evaluating animal models, but accurate assessment in rats presents several challenges. These challenges can be categorized into technical limitations, biological variability, animal care considerations, and potential welfare concerns. High-resolution, high-sensitivity imaging is crucial for accurate measurement. In this study, we employed a hockey stick probe with a cross-section smaller than the width of a rat's neck. This probe design facilitates high-resolution thyroid visualization within the ultrasound equipment. However, individual variations in rats can influence ultrasound wave propagation and reflection, potentially affecting measurement outcomes. To minimize such discrepancies, all measurements in our experiment were conducted on the same platform, with consistent probe angle and positioning relative to the rat's neck. Additionally, we employed lots of coupling gel to mitigate measurement errors arising from probe compression. Animal care and welfare pose a separate challenge during ultrasound examinations. Due to the time-consuming nature of acquiring accurate thyroid measurements (requiring at least three

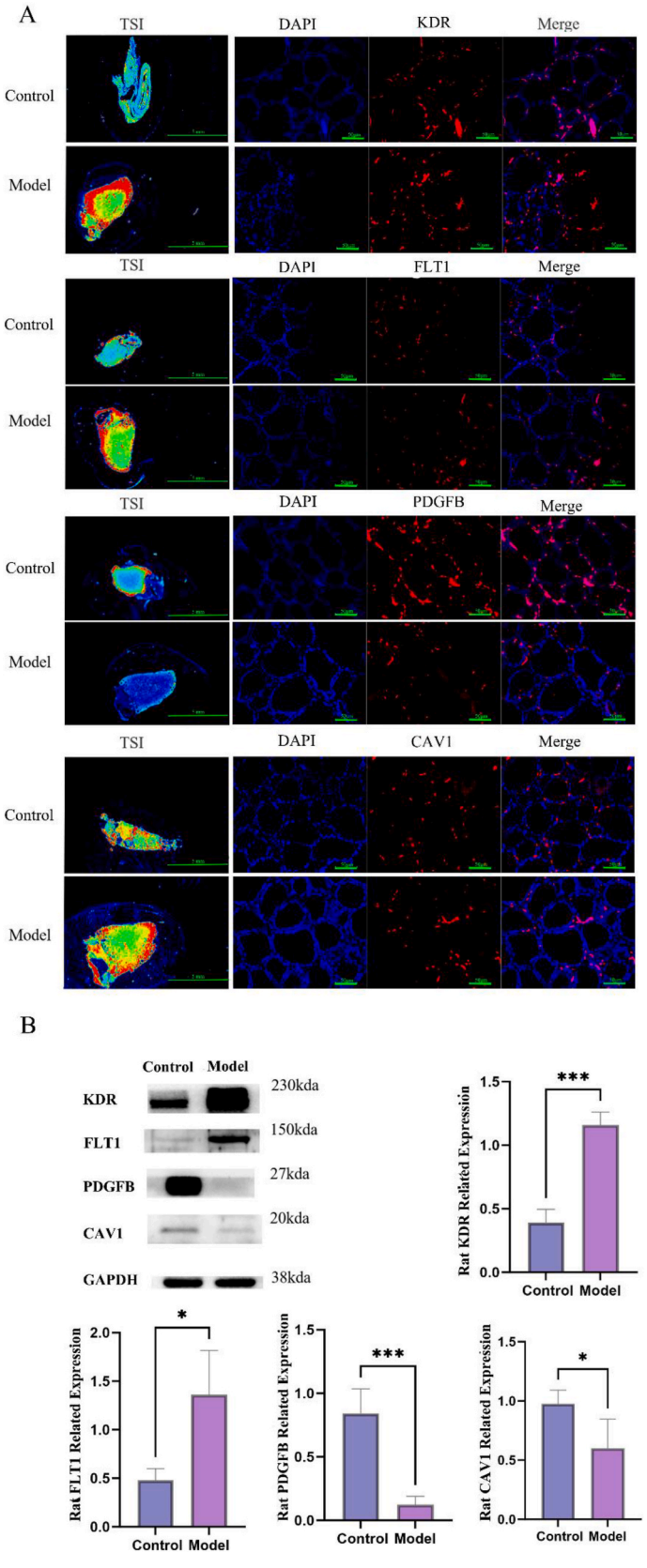

(caption on next page)

Fig. 8. Expression of the key genes KDR, FLT1, PDGFB, and CAV1 in nodular goiter (A) Immunohistochemical section and immunofluorescence analyses were used to detect the effect of the KDR, FLT1, PDGFB and CAV1 proteins in the thyroid tissues of the control group and the model group (Immunohistochemical section scale = 5 mm, n = 3 rats per group, color from blue to red represents the distribution and concentration of related proteins, immunofluorescence scale = 50 μm, magnification × 400, n = 3 rats per group). (B) Western blot detected the KDR, FLT1, PDGFB, CAV1, and GAPDH levels in nodular goiter rats (refer to Supplementary Material 2). Data are shown as the mean ± SD (n = 3). *$P < 0.05$, ***$P < 0.001$ vs. model group. (For interpretation of the references to color in this figure legend, the reader is referred to the Web version of this article.)

measurements per rat), inhalation anesthesia was necessary. We closely monitored the rats' respiratory rate and heart rate throughout the procedure, adjusting the isoflurane flow rate as needed to ensure animal well-being. Our previous studies have established that the PTU-induced, 8-week nodular goiter rat model is stable and suitable for investigation. Furthermore, ultrasonography has been demonstrated as an accurate method for evaluating model development in our previous work [29].

PTU-induced nodular goiter rats displayed a hormonal profile characterized by decreased serum FT3 and FT4 levels alongside elevated TSH levels. These hormonal changes coincided with significant thyroid enlargement. While the control group exhibited a slight upward trend in male thyroid coefficient and TSH levels, histopathological analysis of the model group revealed key diagnostic features of nodular goiter. These features included variation in thyroid follicle size, pronounced epithelial cell proliferation, disorganized follicular architecture, and uneven colloid distribution. Collectively, these findings confirm the successful establishment of a nodular goiter rat model, providing suitable samples for further investigation using RNA-seq technology. RNA-seq is a powerful, high-throughput sequencing technique that offers distinct advantages for studying gene expression in nodular goiter. Unlike traditional methods, RNA-seq enables comprehensive detection of the complete transcriptome, encompassing both known and unknown genes. This comprehensive approach facilitates an in-depth analysis of the gene expression landscape associated with nodular goiter pathogenesis. Additionally, RNA-seq boasts high resolution and accuracy, allowing for the detection of lowly expressed genes and the precise quantification of highly expressed genes within the nodular goiter transcriptome. This powerful technique has the potential to reveal novel gene functions and their contribution to the disease process [30]. Our investigation aimed to elucidate the shared pathogenic mechanisms underlying nodular goiter development in both sexes. The results suggest that common pathogenic

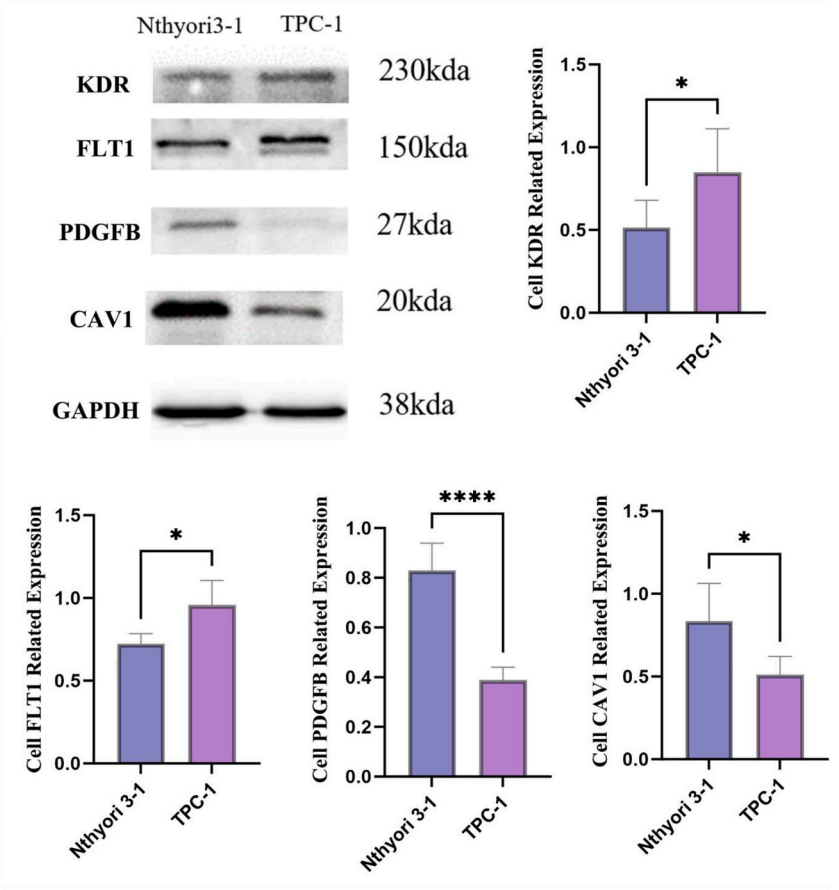

Fig. 9. Validation of the key genes KDR, FLT1, PDGFB, and CAV1 in cells. Data are shown as the mean ± SD (n = 3). *$P < 0.05$, ***$P < 0.001$ vs. model group. The findings from the cellular validation aligned with the results observed in the rats, showing a significant upregulation of KDR and FLT1 expression, while PDGFB and CAV1 expression were notably reduced (refer to Supplementary Material 3).

mechanisms are likely linked to the altered expression of specific genes, including *KDR*, *Flt1*, *PDGFB*, and *CAV1*. Notably, our research not only explored the well-established PI3K-Akt, MAPK, and Ras signaling pathways implicated in nodular goiter but also shed light on lesser-studied pathways in this context, such as the fluid shear stress and atherosclerosis pathway, the calcium signaling pathway, and the Rap1 signaling pathway.

KDR, a receptor tyrosine kinase, plays a critical role in the physiological process of angiogenesis. Ligand binding to KDR serves as the primary signal for initiating angiogenesis. In thyroid pathologies such as thyroiditis and thyroid cancer, KDR expression is upregulated. This increase in KDR expression influences cellular proliferation, vascular growth, and inflammatory processes within the thyroid gland, potentially contributing to the development and recurrence of thyroid tumors. FLT1, another gene encoding a vascular endothelial growth factor (VEGF) receptor, is involved in regulating angiogenesis and has a significant impact on the structural and functional integrity of the thyroid vasculature. CAV1, a major component of caveolae, facilitates the association of integrin subunits with tyrosine kinase molecules.

Several studies have demonstrated a significant upregulation of *KDR* and *FLT1* gene and protein expression in both solitary and recurrent nodular goiter tissues compared to normal thyroid tissue [31]. Additionally, research suggests that elevated TSH levels in PTU-treated rats coincide with a concurrent increase in mRNA and protein levels of PlGF, VEGF, FLT1, and Flk-1/Kd [32]. CAV1, a major component of caveolae, has been identified as an inhibitory regulator of VEGFR receptors. Overexpression of CAV1 leads to a reduction in KDR and FLT1 activities [33,34]. Therefore, given their established roles in regulating angiogenesis and their potential interaction within the context of nodular goiter, KDR, FLT1, and CAV1 are central to our investigation.

Our investigation revealed a significant upregulation of KDR and FLT1 mRNA and protein expression in the experimental group compared to the control group. Conversely, CAV1 expression exhibited an inverse relationship. These findings may be attributed to the elevated TSH levels observed in PTU-induced thyroid nodular tumors. TSH stimulation, mediated through protein kinase A and C signaling pathways, is known to induce increased VEGF production [32,35]. To accommodate this VEGF surge, endothelial cells upregulate KDR and FLT1 receptor abundance while the inhibitory influence of CAV1 on angiogenesis is diminished. This coordinated response results in pronounced vascular congestion within the thyroid gland, potentially promoting cellular proliferation and the development of nodular lesions. Notably, the observed contrast between Nthyori 3–1 and TPC-1 cells warrants further investigation, suggesting a potential link to the progression and worsening of nodular thyroid disease.

A comprehensive literature review did not reveal any prior investigations directly linking *PDGFB* expression to nodular goiter. However, *PDGFB* has been established as a potent angiogenic growth factor, demonstrably promoting neovascularization in dysfunctional murine cardiac tissue through the PDGF-Akt signaling pathway [36]. While these findings may not have a direct implication for nodular goiter pathogenesis, they highlight the critical role of the *PDGFB* system in angiogenesis. Understanding this role is instrumental for elucidating the vascular abnormalities observed in various thyroid diseases, including tumor formation. Therefore, further research specifically focused on PDGF and its potential contribution to nodular goiter development is warranted.

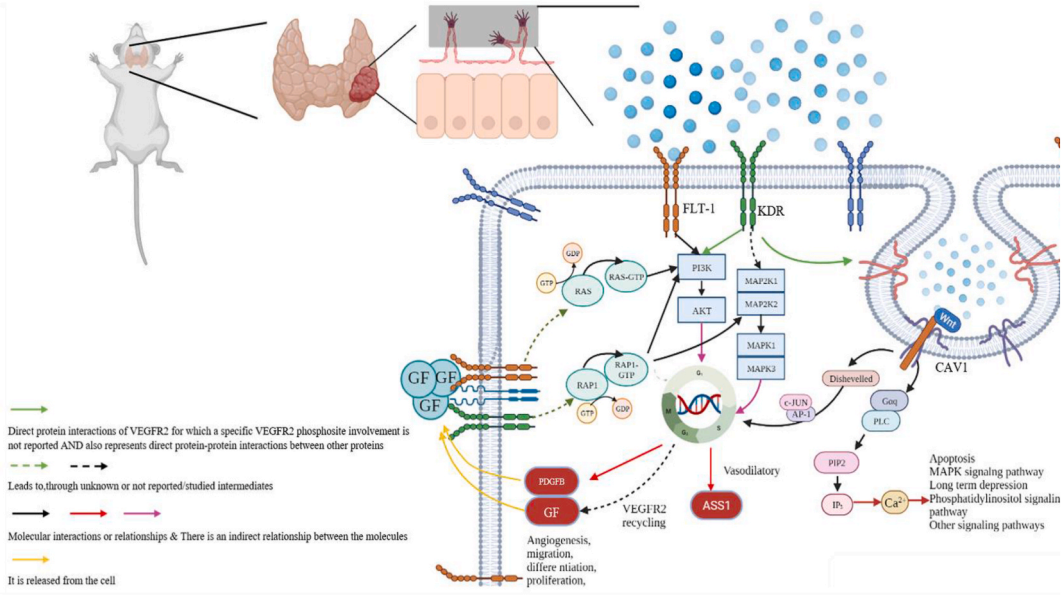

Fig. 10. Pathway distribution of key genes in the occurrence and development of nodular goiter. VEGF, secreted by thyroid follicular epithelial cells, activates signaling cascades by binding to the KDR and FLT1 receptors, which promotes cell proliferation through the PI3K/AKT and MAPK pathways. Additionally, the autocrine secretion of PDGFB by these cells activates the Ras and Rap1 signaling pathways, further enhancing the PI3K/AKT and MAPK pathways. The thyroid's enlargement compresses adjacent blood vessels, inducing fluid shear stress on endothelial cells. This stress leads to changes in KDR expression and function, triggering atherogenic pathways that promote tissue sclerosis and nodule formation within the thyroid. Furthermore, CAV1 modulates the calcium signaling pathways by mitigating effects on KDR and FLT1, affecting the contractility of vascular smooth muscle cells and alterations in pressure, thereby influencing thyroid hemodynamics.

This investigation aimed to elucidate the common pathogenic mechanisms underlying nodular goiter development, irrespective of gender. We propose a model where vascular endothelial growth factors, secreted by thyroid follicular epithelial cells, initiate a signaling cascade. These VEGFs bind to KDR and FLT1 receptors on the cell surface, potentially facilitating transmembrane exchange and activating downstream signaling pathways. Specifically, this initial interaction may trigger the PI3K/AKT and MAPK signaling pathways, which can promote cellular proliferation. Concurrent with VEGF signaling, PDGFB, synthesized by follicular cells, activates the Ras and Rap1 signaling pathways through autocrine signaling via its interaction with various growth factor receptors on the cell membrane. This convergence of signaling pathwaysfurther amplifies the impact of the PI3K/AKT and MAPK pathways, thereby accelerating the process of cellular proliferation associated with nodular goiter [37].

Conversely, an enlarged thyroid gland could compress adjacent blood vessels, altering blood flow velocity and inducing fluid shear stress on the endothelial cells. This stress may modulate the expression and function of KDR, potentially leading to the activation of atherosclerosis pathways. These pathways can promote thyroid tissue stiffening, creating an environment that favors nodule development. Furthermore, under these conditions, CAV1, located within caveolae of the cell membrane, might exhibit a diminished suppressive effect on KDR and FLT1. CAV1 interacts with molecules like nitric oxide synthase and Wnt, thereby initiating calcium signaling pathways that regulate contraction and pressure changes in vascular smooth muscle cells (VSMCs), ultimately influencing the hemodynamics within the thyroid's internal vasculature [38–40]. The activation of these mechanisms not only impacts cellular processes such as the cell cycle, autophagy, and migration, but it may also contribute to the process of thyroid calcification [41–43]. These findings offer novel insights with potential implications for the development of future preventive and therapeutic strategies (Fig. 10).

The findings of our investigation provide compelling evidence supporting the potential role of dysregulated expression of *KDR, FLT1, PDGFB*, and *CAV1* in the pathogenesis of nodular goiter development in both genders. These insights not only expand our understanding of the established pathways involved in nodular goiter but also delve into the potential contributions of novel mechanisms, including fluid shear stress, vascular atherosclerotic processes, calcium signaling pathways, and Rap1 signaling circuits, to disease initiation and progression. These discoveries pave the way for the development of novel therapeutic strategies.

While significant strides have been made in elucidating the shared pathogenic mechanisms of nodular goiter in both sexes using rat models and human cell lines, several key questions remain to be addressed. The rat samples employed for RNA sequencing displayed characteristic features of nodular goiter, as confirmed by both ultrasound and pathological examination. However, the limited sample size precluded definitive identification of all key genes associated with the disease. To compensate for this limitation, we implemented rigorous data analysis techniques to identify genes of potential significance. This approach acknowledges the possibility that additional relevant genes may yet be discovered. Furthermore, due to constraints imposed by the COVID-19 pandemic and the stepwise nature of our study design, RNA sequencing was not performed on human samples. Future research will prioritize the collection of patient samples with confirmed nodular goiter diagnoses. These samples will then be subjected to RNA sequencing and subsequent experimental validation. This strategy will not only facilitate the exploration of common pathogenic mechanisms across genders but also allow for validation of the accuracy of our modeling methods, thereby establishing a robust scientific foundation for future investigations. Finally, our study identified aberrant expression of the *KDR, FLT1, PDGFB,* and *CAV1* genes as critical contributors to the pathogenesis of nodular goiter. However, further exploration of less-investigated pathways, such as those involving fluid shear stress, atherosclerosis, calcium signaling, and Rap1 signaling, is warranted. These pathways have the potential to reveal additional layers of complexity within the disease mechanism and may ultimately lead to the identification of novel therapeutic targets.

5. Conclusions

This investigation explores the shared pathogenic mechanisms underlying nodular goiter development, irrespective of gender. Utilizing both rat models and Nthyori 3–1 and TPC-1 cell lines, we demonstrate that aberrant expression of *KDR, FLT1, PDGFB*, and *CAV1* genes plays a pivotal role in disease initiation in both sexes. Our findings reveal that these gene expression anomalies impact signaling pathways critical for cellular processes, including the PI3K-Akt, MAPK, and Ras pathways, as well as pathways involved in fluid shear stress, atherosclerosis, and calcium signaling. These collective effects culminate in the dysregulation of biological processes such as cell proliferation, angiogenesis, and inflammation, ultimately contributing to the initiation, progression, and exacerbation of nodular goiter. By elucidating the roles of these critical genes and pathways, this study provides essential scientific evidence with the potential to inform the development of novel therapeutic strategies for nodular goiter.

Ethics approval

Laws of the National Institutes of Health-Office of Laboratory Animal Welfare policies and laws. The use of experimental animals has been approved by the Animal Welfare Ethics Review Committee (SDUTCM20230628001) of Shandong University of Traditional Chinese Medicine, and the animals were humanized according to the 3 R principles.

Data availability statement

The datasets used and/or analyzed in the studies presented in this article are available from the corresponding author upon reasonable request.

Consent for publication

All authors have agreed to publish this manuscript.

Funding

This work was supported by the"20 Items for Universities" Funded Project of Ji Nan Science and Technology Bureau [No. 2020GXR002].

CRediT authorship contribution statement

Xiangju Gao: Writing – original draft. **Jie Gao:** Writing – review & editing. **Ya Sun:** Methodology. **Jing Zhao:** Methodology. **Li Geng:** Methodology. **Changlin Wang:** Resources. **Mingqi Qiao:** Resources. **Jieqiong Wang:** Project administration, Funding acquisition, Data curation.

Declaration of competing interest

The authors declare the following financial interests/personal relationships which may be considered as potential competing interests:Jieqiong Wang reports financial support was provided by Ji Nan science and Technology Bureau. If there are other authors, they declare that they have no known competing financial interests or personal relationships that could have appeared to influence the work reported in this paper.

Acknowledgements

We thank the Experimental Center of Shandong University of Traditional Chinese Medicine for providing the experimental site and equipment.

Appendix A. Supplementary data

Supplementary data to this article can be found online at https://doi.org/10.1016/j.heliyon.2024.e33411.

References

[1] M. Knobel, Etiopathology, clinical features, and treatment of diffuse and multinodular nontoxic goiters, J. Endocrinol. Invest. 39 (2016) 357–373, https://doi.org/10.1007/s40618-015-0391-7.
[2] A. Maniakas, L. Davies, M.E. Zafereo, Thyroid disease around the World, Otolaryngol Clin North Am 51 (2018) 631–642, https://doi.org/10.1016/j.otc.2018.01.014.
[3] T. Liu, Y. Li, D. Teng, X. Shi, L. Yan, J. Yang, Y. Yao, Z. Ye, J. Ba, B. Chen, J. Du, L. He, X. Lai, X. Teng, Y. Li, H. Chi, E. Liao, C. Liu, L. Liu, G. Qin, Y. Qin, H. Quan, B. Shi, H. Sun, X. Tang, N. Tong, G. Wang, J.A. Zhang, Y. Wang, Y. Xue, L. Yang, Q. Zhang, L. Zhang, J. Zhu, M. Zhu, Z. Shan, W. Teng, The characteristics of iodine nutrition status in China after 20 Years of universal salt iodization: an epidemiology study covering 31 provinces, Thyroid 31 (2021) 1858–1867, https://doi.org/10.1089/THY.2021.0301.
[4] Y. Li, Z. Shan, W. Teng, Effect of the transition from more than adequate iodine to adequate iodine on national changes in the prevalence of thyroid disorders: repeat national cross-sectional surveys in China, Eur. J. Endocrinol. 186 (2021) 115–122, https://doi.org/10.1530/EJE-21-0975.
[5] I. Yildirim Simsir, S. Cetinkalp, T. Kabalak, Review of factors contributing to nodular goiter and thyroid carcinoma, Med. Princ. Pract. 29 (2020) 1–5, https://doi.org/10.1159/000503575.
[6] G. Accardo, G. Conzo, D. Esposito, C. Gambardella, M. Mazzella, F. Castaldo, C. Di Donna, A. Polistena, N. Avenia, V. Colantuoni, D. Giugliano, D. Pasquali, Genetics of medullary thyroid cancer: an overview, Int. J. Surg. 41 (Suppl 1) (2017) S2–S6, https://doi.org/10.1016/J.IJSU.2017.02.064.
[7] G. Pitsava, C.A. Stratakis, F.R. Faucz, PRKAR1A and thyroid tumors, Cancers 13 (2021), https://doi.org/10.3390/cancers13153834.
[8] J.A. Baran, S. Halada, A.J. Bauer, J.C. Ricarte-Filho, A. Isaza, L.F. Surrey, C. McGrath, T. Bhatti, J. Jalaly, S. Mostoufi-Moab, A.T. Franco, N.S. Adzick, K. Kazahaya, A.M. Cahill, Z. Baloch, Indeterminate thyroid fine-needle aspirations in pediatrics: exploring clinicopathologic features and utility of molecular profiling, Horm. Res. Paediatr. 95 (2022) 430–441, https://doi.org/10.1159/000526116.
[9] K. Van Der Tuin, L. De Kock, E.J. Kamping, S.E. Hannema, M.J.M. Pouwels, M. Niedziela, T. Van Wezel, F.J. Hes, M.C. Jongmans, W.D. Foulkes, H. Morreau, Clinical and molecular characteristics may alter treatment strategies of thyroid malignancies in DICER1 syndrome, J. Clin. Endocrinol. Metab. 104 (2019) 277–284, https://doi.org/10.1210/JC.2018-00774.
[10] Y. Li, C. Jin, J. Li, M. Tong, M. Wang, J. Huang, Y. Ning, G. Ren, Prevalence of thyroid nodules in China: a health examination cohort-based study, Front. Endocrinol. 12 (2021), https://doi.org/10.3389/FENDO.2021.676144/PDF.
[11] M. Yadav, V. Kose, A. Bhalerao, Frequency of thyroid disorder in pre- and postmenopausal women and its association with menopausal symptoms, Cureus 15 (2023), https://doi.org/10.7759/cureus.40900.
[12] L. Wang, L. Zhao, X. Jia, L. Jiang, Y. Song, Q. Ye, Z. Lyu, Aminophenols increase proliferation of thyroid tumor cells by inducing the transcription factor activity of estrogen receptor α, Biomed. Pharmacother. 109 (2019) 621–628, https://doi.org/10.1016/J.BIOPHA.2018.10.168.
[13] R. Rahbari, L. Zhang, E. Kebebew, Thyroid cancer gender disparity, Future Oncol. 6 (2010) 1771–1779, https://doi.org/10.2217/FON.10.127.
[14] Juan Wu, F.E.N.G. Hongfang, L.I. Xiang, C.H.E.N. Chuang, Shan Zhu, Shengrong Sun, Clinical and pathological analysis of 1358 patients with thyroid nodules, J Clin Surgery 24 (2016) 197–200, https://doi.org/10.3969/j.issn.1005-6483.2016.03.012.
[15] Xiaomei Zhang, Yanfei Kang, Tian Sang, Jing Cheng, L.I. Qiaoli, Yuwen Cao, Jinmei Ma, S.H.I. Linan, L.I. Wenxiao, LI jun, predictive value of combined use of ultrasonographic indicators for central lymph node metastasis in papillary thyroid carcinoma, Chinese General Practice 25 (2022) 305–311, https://doi.org/10.12114/j.issn.1007-9572.2021.02.109.

[16] M. Griessen, T. Lemarchand-Béraud, Thyrotropin secretion and metabolism in rats during propylthiouracil treatment, Endocrinology 92 (1973) 166–173, https://doi.org/10.1210/ENDO-92-1-166.
[17] C. Casella, R. Morandi, A. Verrengia, A. Galani, S. Molfino, D. Cuka, G. Groppo, C. Cappelli, N. Portolani, Thyroid cancer and nodules in Graves' disease: a single center experience, Endocr., Metab. Immune Disord.: Drug Targets 21 (2021) 2028–2034, https://doi.org/10.2174/1871530321666201230111911.
[18] I. Hassan, H. El-Masri, J. Ford, A. Brennan, S. Handa, K. Paul Friedman, M.E. Gilbert, Extrapolating in vitro screening assay data for thyroperoxidase inhibition to predict serum thyroid hormones in the rat, Toxicol. Sci. 173 (2020) 280–292, https://doi.org/10.1093/TOXSCI/KFZ227.
[19] B.R. Haugen, E.K. Alexander, K.C. Bible, G.M. Doherty, S.J. Mandel, Y.E. Nikiforov, F. Pacini, G.W. Randolph, A.M. Sawka, M. Schlumberger, K.G. Schuff, S. I. Sherman, J.A. Sosa, D.L. Steward, R.M. Tuttle, L. Wartofsky, American thyroid association management guidelines for adult patients with thyroid nodules and differentiated thyroid cancer: the American thyroid association guidelines task force on thyroid nodules and differentiated thyroid cancer, Thyroid 26 (2016) (2015) 1–133, https://doi.org/10.1089/THY.2015.0020.
[20] K. Pazaitou-Panayiotou, K. Michalakis, R. Paschke, Thyroid cancer in patients with hyperthyroidism, Horm. Metab. Res. 44 (2012) 255–262, https://doi.org/10.1055/S-0031-1299741.
[21] M.I. Abdullah, S.M. Junit, K.L. Ng, J.J. Jayapalan, B. Karikalan, O.H. Hashim, Papillary thyroid cancer: genetic alterations and molecular biomarker investigations, Int. J. Med. Sci. 16 (2019) 450–460, https://doi.org/10.7150/IJMS.29935.
[22] M. Tamura, H. Kimura, T. Koji, T. Tominaga, K. Ashizawa, T. Kiriyama, N. Yokoyama, T. Yoshimura, K. Eguchi, P.K. Nakane, S. Nagataki, Role of apoptosis of thyrocytes in a rat model of goiter. A possible involvement of Fas system, Endocrinology 139 (1998) 3646–3653, https://doi.org/10.1210/ENDO.139.8.6140.
[23] Y. Wang, C. Li, Z. Xiong, N. Chen, X. Wang, J. Xu, Y. Wang, L. Liu, H. Wu, C. Huang, A. Huang, J. Tan, Y. Li, Q. Li, Up-and-coming anti-epileptic effect of aloesone in Aloe vera: evidenced by integrating network pharmacological analysis, in vitro, and in vivo models, Front. Pharmacol. 13 (2022), https://doi.org/10.3389/FPHAR.2022.962223/PDF.
[24] H. Wang, Y. Jiang, J. Song, H. Liang, Y. Liu, J. Huang, P. Yin, D. Wu, H. Zhang, X. Liu, D. Zhou, W. Wei, L. Lei, J. Peng, J. Zhang, The risk of perchlorate and iodine on the incidence of thyroid tumors and nodular goiter: a case-control study in southeastern China, Environ. Health 21 (2022), https://doi.org/10.1186/S12940-021-00818-8.
[25] X.I.A. Zongxiao, L.I.U. Haipeng, Yanjiao Zhang, Yuan Fan, Research progress on animal models of thyroid disease, Chin. J. Comp. Med. 32 (2022) 87–93, https://doi.org/10.3969/j.issn.1671-7856.2022.02.013.
[26] J. Sun, C. Hui, T. Xia, M. Xu, D. Deng, F. Pan, Y. Wang, Effect of hypothyroidism on the hypothalamic-pituitary-ovarian axis and reproductive function of pregnant rats, BMC Endocr. Disord. 18 (2018), https://doi.org/10.1186/S12902-018-0258-Y.
[27] A. Alayoubi, R.D. Sullivan, H. Lou, H. Patel, T. Mandrell, R. Helms, H. Almoazen, In vivo evaluation of transdermal iodide microemulsion for treating iodine deficiency using sprague dawley rats, AAPS PharmSciTech 17 (2016) 618–630, https://doi.org/10.1208/S12249-015-0392-Z.
[28] J. Li, Z. Liu, H. Zhao, F. Yun, Z. Liang, D. Wang, X. Zhao, J. Zhang, H. Cang, Y. Zou, Y. Li, Alterations in atrial ion channels and tissue structure promote atrial fibrillation in hypothyroid rats, Endocrine 65 (2019) 338–347, https://doi.org/10.1007/S12020-019-01968-Z.
[29] Xiangju Gao, Dongmei Gao, Xianmei Chen, Tingting Song, Zhan Gao, Jie Gao, Jieqiong Wang, Ultrasound imaging for evaluation of nodular goiter in rats, Chin. J. Comp. Med. 33 (2023) 78–84+118, https://doi.org/10.3969/j.issn.1671-7856.2023.01.010.
[30] G.W. Wilson, L.D. Stein, RNASequel: accurate and repeat tolerant realignment of RNA-seq reads, Nucleic Acids Res. 43 (2015), https://doi.org/10.1093/NAR/GKV594.
[31] N.H. Mohamad Pakarul Razy, W.F.W.A. Rahman, T.T. Win, Expression of vascular endothelial growth factor and its receptors in thyroid nodular hyperplasia and papillary thyroid carcinoma: a tertiary health care centre based study, Asian Pac. J. Cancer Prev. APJCP 20 (2019) 277–282, https://doi.org/10.31557/APJCP.2019.20.1.277.
[32] K. Sato, K. Yamazaki, K. Shizume, Y. Kanaji, T. Obara, K. Ohsumi, H. Demura, S. Yamaguchi, M. Shibuya, Stimulation by thyroid-stimulating hormone and Grave's immunoglobulin G of vascular endothelial growth factor mRNA expression in human thyroid follicles in vitro and flt mRNA expression in the rat thyroid in vivo, J. Clin. Invest. 96 (1995) 1295–1302, https://doi.org/10.1172/JCI118164.
[33] L. Labrecque, I. Royal, D.S. Surprenant, C. Patterson, D. Gingras, R. Béliveau, Regulation of vascular endothelial growth factor receptor-2 activity by caveolin-1 and plasma membrane cholesterol, Mol. Biol. Cell 14 (2003) 334–347, https://doi.org/10.1091/MBC.E02-07-0379.
[34] B. Vasir, J.-C. Jonas, G.M. Steil, J. Hollister-Lock, W. Hasenkamp, A. Sharma, S. Bonner-Weir, G.C. Weir, Gene expression of VEGF and its receptors Flk-1/KDR and Flt-1 in cultured and transplanted rat islets, Transplantation 71 (2001) 924–935, https://doi.org/10.1097/00007890-200104150-00018.
[35] B.J. Morris, R. Chen, T.A. Donlon, K.J. Kallianpur, K.H. Masaki, B.J. Willcox, Vascular endothelial growth factor receptor 1 gene (FLT1) longevity variant increases lifespan by reducing mortality risk posed by hypertension, Aging 15 (2023) 3967–3983, https://doi.org/10.18632/aging.204722.
[36] J. Chen, S.B. Ortmeier, O.V. Savinova, V.B. Nareddy, A.J. Beyer, D. Wang, A.M. Gerdes, Thyroid hormone induces sprouting angiogenesis in adult heart of hypothyroid mice through the PDGF-Akt pathway, J. Cell Mol. Med. 16 (2012) 2726–2735, https://doi.org/10.1111/J.1582-4934.2012.01593.X.
[37] R. Wu, S. Gandhi, Y. Tokumaru, M. Asaoka, M. Oshi, L. Yan, T. Ishikawa, K. Takabe, Intratumoral PDGFB gene predominantly expressed in endothelial cells is associated with angiogenesis and lymphangiogenesis, but not with metastasis in breast cancer, Breast Cancer Res. Treat. 195 (2022) 17–31, https://doi.org/10.1007/S10549-022-06661-W.
[38] J. Ma, Y. Li, X. Yang, K. Liu, X. Zhang, X. Zuo, R. Ye, Z. Wang, R. Shi, Q. Meng, X. Chen, Signaling pathways in vascular function and hypertension: molecular mechanisms and therapeutic interventions, Signal Transduct. Targeted Ther. 8 (2023), https://doi.org/10.1038/S41392-023-01430-7.
[39] F. Moccia, S. Negri, M. Shekha, P. Faris, G. Guerra, Endothelial Ca2+ signaling, angiogenesis and vasculogenesis: just what it takes to make a blood vessel, Int. J. Mol. Sci. 20 (2019), https://doi.org/10.3390/ijms20163962.
[40] P. Agretti, G. De Marco, E. Ferrarini, C. Di Cosmo, L. Montanelli, B. Bagattini, L. Chiovato, M. Tonacchera, Gene expression profile in functioning and non-functioning nodules of autonomous multinodular goiter from an area of iodine deficiency: unexpected common characteristics between the two entities, J. Endocrinol. Invest. 45 (2022) 399–411, https://doi.org/10.1007/S40618-021-01660-Y.
[41] S. Bhattacharya, R.K. Mahato, S. Singh, G.K. Bhatti, S.S. Mastana, J.S. Bhatti, Advances and challenges in thyroid cancer: the interplay of genetic modulators, targeted therapies, and AI-driven approaches, Life Sci. 332 (2023), https://doi.org/10.1016/J.LFS.2023.122110.
[42] Y. He, X.Y. Wang, Q. Hu, X.X. Chen, B. Ling, H.M. Wei, Value of contrast-enhanced ultrasound and acoustic radiation force impulse imaging for the differential diagnosis of benign and malignant thyroid nodules, Front. Pharmacol. 9 (2018), https://doi.org/10.3389/fphar.2018.01363.
[43] M.Y. Asghar, T. Lassila, K. Törnquist, Calcium signaling in the thyroid: friend and foe, Cancers 13 (2021), https://doi.org/10.3390/CANCERS13091994.